Numerical modelling of elastohydrodynamic lubrication in soft contacts using non-Newtonian fluids

M.F.J. Bohan, I.J. Fox, T.C. Claypole and D.T. Gethin
Department of Mechanical Engineering, University of Wales, Swansea, UK

Keywords *Lubrication, Non-Newtonian fluids*

Abstract *The paper focuses on the solution of a numerical model to explore the sliding and non-Newtonian fluid behaviour in soft elastohydrodynamic nip contacts. The solution required the coupling of the fluid and elastomer regimes, with the non-Newtonian fluid properties being described using a power law relationship. The analysis showed that the fluid characteristics as defined by the power law relationship led to large differences in the film thickness and flow rate with a movement of the peak pressure within the nip contact. The viscosity coefficient, power law index and sliding ratio were shown to affect the nip performance in a non-linear manner in terms of flow rate and film thickness. This was found to be controlled principally by the level of viscosity defined by the power law equation. The use of a speed differential to control nip pumping capacity was also explored and this was found to be most sensitive at lower entrainment speeds.*

Introduction

Many coating processes consist of a number of rollers that form a train to meter accurately and consistently the transfer of a small amount of fluid onto a substrate to form a thin coating (Kistler and Schweizer, 1997). In such systems, alternating rubber covered and steel rollers make up the roller train, Figure 1, and the roller speeds are set to establish a significant component of sliding in the nip junction. The contacts between the rollers normally have a positive engagement that is facilitated by deformation of the elastomer surface. In addition, at each roller contact, fluid pressure will also deform the rubber surface, which in turn will affect the hydrodynamic pressure that is generated within the contact. For the purpose of simulation, this leads to the requirement for an iterative approach in solution, linking the fluid field model with the elastic deformation of the rubber cover. This is usually referred to as Soft Elasto Hydrodynamic Lubrication (SEHL) and since the rollers are long in comparison with the junction width, the geometry reflects a line contact.

The authors wish to acknowledge the financial support of EPSRC through the award of a platform grant.

International Journal of Numerical Methods for Heat & Fluid Flow, Vol. 12 No. 4, 2002, pp. 494-511.

DOI 10.1108/09615530210433297

Roller nip interaction can be classified as a contact problem. This class of problem has been reported widely in the literature, however the following will focus on studies that are relevant to this investigation.

Analysis of the behaviour of a roller pair using experimental or numerical approaches has been reported for both dry and wet contacts in which one or more surfaces is soft and therefore compliant. One of the first (Hannah, 1951), which has formed the basis of much subsequent analysis, considered the contact between narrow discs. These discs comprised one rigid surface and the second covered with a soft material and they were placed in positive engagement. The integral equations used the Hertzian theory to define the pressure distribution within the contact and calculations were carried out for roller coverings having both thin and thick compliant layers. These early results highlighted the importance of the layer thickness and contact width.

This numerical scheme was subsequently developed (Parish, 1958; Miller, 1966) from the plane stress, narrow disc model to a plane strain approach that is pertinent to roller contact analysis. The papers have assessed the influence of many parameters including layer thickness, elastic modulus, roller radius, Poisson's ratio and speed differentials. Results indicated that while the Poisson's ratio affected the deformation shape, reflecting the level of incompressibility of the covering, the thickness affected the degree of deformation.

The above work has considered dry contacts only, one of the first studies of wet contacts (Bennett and Higginson, 1970) analysed a hard roller rotating against a polythene target. This used a simple linear elastic deformation model based on the local pressure and stiffness of the polythene target, the coupling of which allowed the impact of friction to be evaluated in this simple sliding contact. Analysis of heavily loaded contacts has been reported in Hooke and O'Donoghue (1972). This used parabolic functions to express the pressure in the inlet and outlet regions, blending this with a pressure profile based on a dry Hertzian contact in the central region. The influence of the contact width to layer thickness ratio was evaluated showing that as it increased so did the peak pressure, again confirming the importance of the layer thickness.

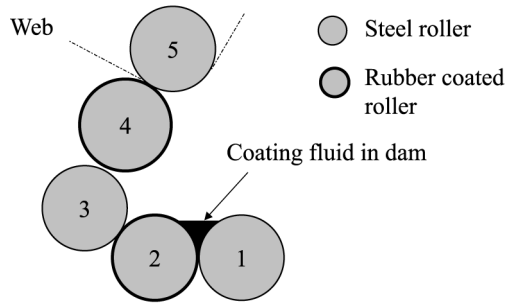

Figure 1.
Schematic of a multiple roller coating application

The requirement to iterate between the fluid and elastomer regions in the numerical solution for SEHL problems was highlighted in Cudworth (1979) in which the authors employed a finite element approach to solve the governing equations. Again this work confirmed that the film thickness and pressure profiles were influenced dominantly by layer thickness and load. This result was also confirmed in Hooke (1986) when the authors explored the effect of inlet conditions replicating the extent of flooding in the nip.

The preceding works have generally focused on tribology applications. Limited analysis has been carried out into the application of these methods to printing (MacPhee *et al.*, 1992; Bohan *et al.*, 1997). The first (MacPhee *et al.*, 1992) assessed the impact of the inlet conditions, flooded or starved, on the nip and this showed large differences in the performance when these were altered, supporting the results presented in Hooke (1986). The second (Bohan *et al.*, 1997b) adopted a more fundamental approach in which the elastomer deformation was computed from a basic elastic analysis. This effectively allowed exploration of the basic assumption that a Hertzian contact model is applicable. In terms of pressure profile, the analysis showed a favourable comparison in form with experimental data and a close match could be achieved when an appropriate Young's Modulus was chosen. This analysis also showed that the pressure in the nip departed from a Hertzian form, reflecting a hydrodynamic profile and a tapering film thickness. Calculations were also carried out to explore the impact of nip geometry and engagement conditions and this showed that increasing the contact width increased both the pressure and film thickness.

Consideration of coating applications is more recent and the work in Carvalho and Scriven (1997) includes a comprehensive review of relevant work and also details a combined modelling and experimental programme. The numerical scheme adopts a Hertzian contact model to compute deformation in the contact and this is coupled with the solution of the hydrodynamic pressure in the film, based on a Newtonian fluid. Elastomer deformation is based on a simple linear spring model. Of particular interest in this work is the application of a Landau-Levich film rupture model that incorporates a surface tension mechanism in the film splitting zone. Consequently it is capable of capturing the subambient pressure that has been measured in the nip (Bohan *et al.*, 1997b; Carvalho and Scriven, 1997). Case studies were run off for which there is no positive engagement and deformation of the elastomer is due to hydrodynamic action alone. From the steady state analysis, the most important result is that the soft elastomer layer leads to a film splitting location that is less dependent on roller position for smaller gaps. This is significant since it also makes the nip pumping capacity nearly independent of roller position for small gaps for which precise settings are difficult to achieve. The study also includes an unsteady analysis via a perturbation model to explore the conditions under which cavitation fingers are developed in the nip exit region and to establish

conditions under which they can be eliminated from the system. The results also show the importance of a soft layer in delaying the onset of ribbing instabilities.

A number of investigations have been carried out by several authors to evaluate the influence of non-Newtonian fluid behaviour in both rolling and sliding contacts. A recent review of this type of work is presented in Dowson and Ehret (1999). This showed that many of these studies have focused on transmission components where rolling action is common and in which the pressures are high and the lubricant is treated as a piezoviscous fluid. Fewer studies have been carried out focusing on the exploration of shear rate dependent behaviour. One of the most important conclusions stated in Dowson and Ehret (1999) is the need to treat "real" surface and fluid systems and that this should be a thrust of future research work.

The use of a power law to express the shear thinning behaviour of the fluid introduces numerical difficulties, since it infers an extremely high (infinite) viscosity at very low shear rates. Similarly the application of an upper shear rate may be used to prevent the fluid viscosity falling below a set level. The latter does not introduce numerical difficulties, but is driven by the process of validation against experimental measurement. An example of the use of an upper shear limit on the behaviour of the fluid is presented in Jacobson and Hamrock (1984). The limit was utilised allowing analysis using a power law expression within an operational envelope, beyond which, a Newtonian model was applied. This was demonstrated through application to a hard EHL contact for which the effect of fluid behaviour on the nip pressures and film thickness was calculated. This showed that the influence of non-dimensional speed and shear strength had only a small impact on the minimum film thickness.

An early study of SEHL in a rolling contact for a power law fluid (Lim *et al.*, 1996) was used in the exploration of a printing application in which near pure rolling takes place. Shear rate cut-off values were used to avoid numerical singularities under conditions where the shear rate approached a zero value. The importance of both the power law co-efficient and exponents on the nip performance was quantified. This showed significant impacts for both parameters, with increases in each resulting in increased film thickness and maximum pressure.

The purpose of this paper is to explore the application of numerical simulation to coating applications that involve combined sliding and rolling mechanisms. This will extend previous work (Carvalho and Scriven, 1997; Lim *et al.*, 1996) through the incorporation of actual fluid properties that exhibit shear thinning and it will also include nip configurations in which there is positive engagement. Through case studies the effect of the power law co-efficient, power law exponent and sliding on the nip performance in terms of

pressure distribution, film thickness profile, strain rate and viscosity variation through the nip section and flow rate will be investigated.

Theoretical model background

The solution of the soft elastohydrodynamic lubrication contact is obtained by coupling the solution of the fluid film equations with those describing the mechanical deformation of the surfaces. The behaviour is coupled since the film thickness determines the pressure variation in the junction and this is established in the fluid domain calculation. In turn, the pressure variation defines the rubber deformation attributed to hydrodynamic action (Cudworth, 1979) and this is computed within the structural model. This dictates the need for iteration between the fluid and structural domains within the overall solution process. The basic equations together with their solution strategy will be discussed in the following sections, including the approach for handling the non-Newtonian fluid behaviour.

Elastic deformation

Since the deformation at the roller surface is small, the displacement of the rubber layer on the roller may be assumed to be linearly elastic. The deformation of this roller may be established using a number of numerical schemes. In the present study only the deformation of the surface is of interest and this is derived economically by using a boundary element approach. For a plain strain case, the boundary element integral equation for the solution of the general problem of elasticity under steady loading is given by Brebbia and Dominguez (1989):

$$c^i_{lk} u^i_k + \int_\Gamma p^*_{lk} u_k \ \mathrm{d}\Gamma = \int_\Gamma u^*_{lk} p_k \ \mathrm{d}\Gamma + \int_\Omega u^*_{lk} b_k \ \mathrm{d}\Omega \tag{1}$$

In coating applications, the speeds are modest and so centrifugal effects are negligible. Thermal effects may also be present in the nip. Sources are localised and include the shearing of the fluid film and deformation within the elastomer structure. The film is thin and therefore the shear stresses are high. However, the narrowness of the contact (typically 6 mm) is likely to be insufficient to allow any significant temperature build up to take place. Also the thermal capacity of the fluid is high, typically an oil based coating has a density of 900 kg/m^3 and a specific heat capacity of 2000 J/kg°C and this is also likely to ensure that the heating effect of fluid shearing is small. Similarly the energy dissipation in the elastomer will be low due to small engagements and low speed. Operating experience shows that elastomer heating becomes important when multiple rigid rollers are in contact with a single rubber covered roller. This leads to catastrophic failure of the rubber roller at high running speeds (e.g 700 m/min). This suggests that local thermal influence will be small and therefore the equation can be written as:

$$c^i_{lk}u^i_k + \int_\Gamma p^*_{lk}u_k \ \mathrm{d}\Gamma = \int_\Gamma u^*_{lk}p_k \ \mathrm{d}\Gamma \tag{2}$$

The discretisation of this equation will be explained below in the solution procedure section.

Generalised pressure equation

For a non-Newtonian fluid flow the thin film equations are derived accounting for the variation of viscosity, leading to a generalised pressure equation (Dowson, 1962). Provided that the analysis plane is some distance from the roller edge then this equation can be written in a one-dimensional form as:

$$\frac{\mathrm{d}}{\mathrm{d}x}\left[G\frac{\mathrm{d}p}{\mathrm{d}x}\right] = U_2\left[\frac{\mathrm{d}h}{\mathrm{d}x}\right] + (U_1 - U_2)\left[\frac{\mathrm{d}F}{\mathrm{d}x}\right] \tag{3}$$

where

$$G = \int_0^h \frac{y}{\mu}(y - F)\mathrm{d}y \tag{4}$$

$$F_1 = \int_0^h \frac{y}{\mu}\mathrm{d}y; \ \ F_0 = \int_0^h \frac{1}{\mu}\mathrm{d}y; \ \ F = \frac{F_1}{F_0} \tag{5}$$

The integrals can be evaluated and the pressure equation (3) solved for a non-Newtonian fluid once the variation of viscosity (μ) due to the combination of Poiseuille and Couette flow is known over the film thickness. This governing equation was solved using a finite difference numerical scheme and nodal pressure convergence within 10^{-6} Pa between successive iterations was assigned.

The viscosity field can be established either via the solution of a complex set of equations (Walters, 1975) or more simply by means of a power law equation (Wilkinson, 1960), where the shear stress is related to velocity gradient via the equation

$$\tau = m\left|\frac{\mathrm{d}u}{\mathrm{d}y}\right|^{n-1}\frac{\mathrm{d}u}{\mathrm{d}y} \tag{6}$$

The term $m|\mathrm{d}u/\mathrm{d}y|^{n-1}$ effectively represents the viscosity coefficient and for a Newtonian fluid, $n = 1$ and m is the dynamic viscosity. When $n < 1$, the fluid shear thins and assumes a pseudoplastic form. The determination of viscosity through the film relies on the calculation of the local velocity gradient and these may be determined through numerical differentiation of the velocity profile. Such profiles also need to account for the cross film viscosity variation and therefore the velocity variation was derived using equation (7). This equation

embodies the velocity boundary condition that the fluid adheres to each roller surface and therefore moves at their respective surface velocities U_1 and U_2.

$$u(\alpha) = U_1 + \frac{\mathrm{d}p}{\mathrm{d}x}\int_0^\alpha \frac{y}{\mu}\mathrm{d}y + \left(\frac{U_2 - U_1}{F_0} - \frac{F_1}{F_0}\frac{\mathrm{d}p}{\mathrm{d}x}\right)\int_0^\alpha \frac{\mathrm{d}y}{\mu} \tag{7}$$

Since equation (7) includes a cross film variation of viscosity through the terms F (see Equation (5)) it needs to be solved iteratively. This was implemented within the solution algorithm with a close tolerance on viscosity at each point through the film. Typically convergence to within 10^{-4} Pas between successive iterations was satisfied. For more extreme conditions it was also necessary to introduce damping into the solution to ensure stability.

The integration of this equation into the overall solution procedure will be described in a following section.

Film thickness

Closure of the equation set requires a definition of film thickness. This was expressed using the following equation that embodies an equivalent roller radius. A negative value of h_0 indicates a roller engagement and the term $u(x)$ represents the local deformation of the elastomer layer.

$$h(x) = h_0 + \frac{x^2}{2R} + u(x) \tag{8}$$

Load

The solution strategy seeks to modify the film thickness profile to satisfy a load application constraint and completion of the solution was obtained when the computed load meets the set value, to a tolerance, T_l, of less than 0.1 per cent.

$$\left|\left[\int_{x_1}^{x_2} p.\mathrm{d}x\right] - L\right| \leq T_l * L \tag{9}$$

Solution procedure

The thin film model embodies the assumption that the elastomer may be unwrapped to give a flat surface in the locality of the contact. Previous analysis (Dowson and Higginson, 1959) has been carried out to compare results from a flat (unwrapped) model and a model that includes curvature, representing the actual roller. The latter does not use linear elements and therefore requires a numerical integration of the boundary elements. This extends the calculation duration. The work in Dowson and Higginson (1959) has shown that this has a negligible effect on the predicted deformation. The boundary of the elastomer was divided into a number of linear elements, Figure 2, from which to obtain the integrals in the elasticity equation. The use of linear elements in a finite plane model allows the element integrals to be calculated analytically. As well

as allowing a rapid solution, this allows elements to be formulated that are suited to a solution with a Poisson's ratio of 0.5 (Brebbia and Dominguez, 1989; Banerjee and Butterfield, 1981), avoiding the numerical singularity that is usually present with this material property specification. Consistent with the elastomer mesh, the fluid domain was solved over the nip contact, X_a to X_b.

Following extensive exploration of solution strategies, the following steps have been established to give an accurate and stable result.

(1) Define the mesh over the elastomer boundary and calculate the division for the fluid side calculations.

(2) Set an initial value for the engagement, h_0, from this the Hertzian pressure and the consequent deformation is calculated.

(3) Calculate the film thickness in the nip junction.

(4) Solve for the film pressure, including iteration for non-Newtonian behaviour.

(5) Recalculate the elastomer deformation.

(6) If the deformation has not met the convergence criteria, then repeat from stage (3) with the new deformation.

(7) Once the deformation criterion has been met, examine the load equilibrium. If this is not met then appoint a new value for h_0 and repeat from (2).

The convergence requirement for the analysis was 0.1 percent on the pressure and indentation. Convergence of the solutions was usually obtained in approximately 5,000 iterations.

Results and discussion

A typical industrial configuration was used in the study to illustrate the application of the model described above. It is based on a coating application where the rollers run at different surface speeds thereby introducing a sliding component as a method to control the flow rate through the nip. The roller parameters and loading condition are itemised in Table I and have been derived from process data and the elastic modulus from material property measurement. Within the calculation different roller speeds as well as different power law exponents will be explored and these will be defined accordingly.

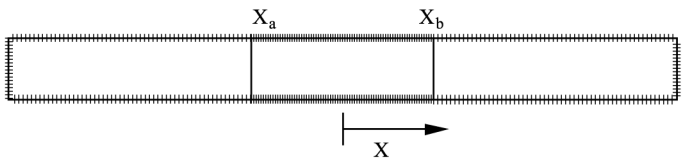

Figure 2.
Schematic discretisation of the elastomer layer

The actual fluid properties of a typical ink has been characterised using a cone and plate rheometer from which the relationship between shear stress and shear rate has been quantified (Lim *et al.*, 1996). This provides indicative values. Some coating fluids are noted to be highly viscous systems, exhibiting similar consistency. Using this information, the parameters for a power law fluid have been determined and appropriate values give a dynamic viscosity coefficient (m) of 50 and an exponent value (n) of 0.75. These have been used as a starting point for the investigation to evaluate the impact of changing from a Newtonian to non-Newtonian fluid and to explore the variations as a consequence of using different power law coefficients and exponents. As explained in the review, a lower cut-off in shear rate value needs to be used to avoid singularity in the determination of viscosity over the film thickness. An inappropriate choice can mask the shear-thinning model and therefore a range of values from 100/s to 500/s was explored. The results in terms of nip flow rate were virtually identical and therefore a cut-off of 250/s was finally chosen and this leads to a lower viscosity of limit of 12.57 Pas. This value was used in all calculations for Newtonian flow that serve as a benchmark with which to explore the effect of non-Newtonian behaviour.

Influence of non-Newtonian characteristics on nip performance

Initial calculation was carried out for a pure rolling nip in which the surface velocity was 2.5 m/s for both rollers. The results from this calculation are displayed in Figure 3 as pressure and film thickness profiles through the nip. Significant differences in the film thickness profiles and small differences in the form of the pressure profile may be noted. The latter clearly satisfies the over all load constraint of equation (9). For the non-Newtonian fluid, the pressure peak moves nearer to the nip centre and achieves a slightly higher value. At this point the fluid achieves a Newtonian level because the velocity gradients through the film are negligible (see Figure 4). In the absence of a pressure gradient, the velocity profile represents a simple plug flow when the rollers forming the nip rotate to give identical surface velocities.

The changes in minimum film thickness are much more dramatic. Over the nip contact there is significant shear thinning and this leads to a 27.4 per cent reduction in minimum film thickness. The pumping capacity is determined by the film thickness at which the pressure gradient is zero and the entraining

Table I. Roller parameter details

Parameter	Conditions
Load (Nm^{-1})	7000
Roller radius (m)	0.15
Elastic modulus (Pa)	2.0e+6
Rubber thickness (mm)	15

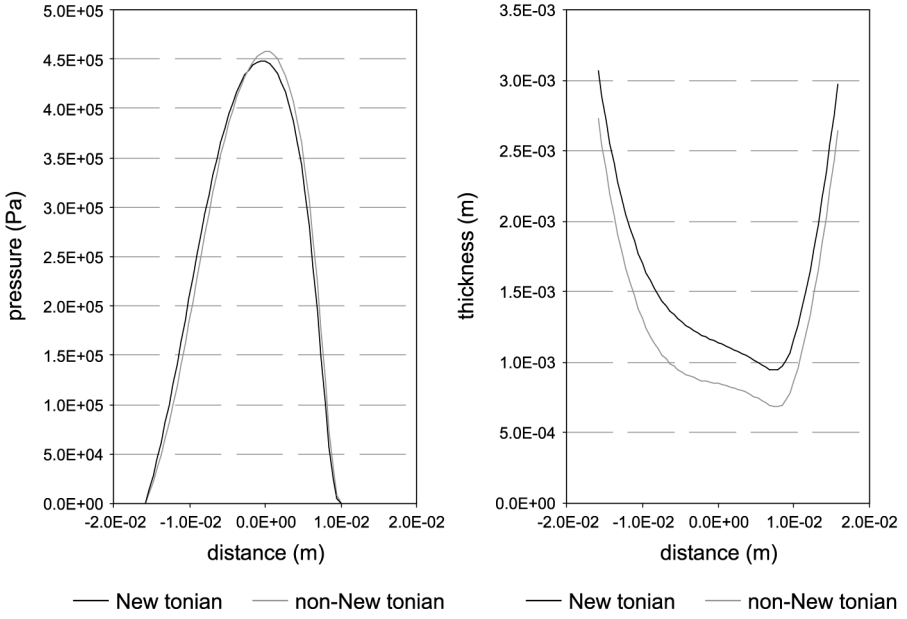

Figure 3.
Influence of non-Newtonian behaviour on the pressure profile and film thickness

velocity of the two roller surfaces. Since the point of zero pressure gradient occurs close to the point of minimum film thickness, the nip shows a commensurate reduction of 26.4 per cent in its pumping capacity. This result has an important practical implication when coating systems are set according to roller load. The shear thinning mechanism leads to a reduction in film thickness and a reduction in coating weight as a consequence.

The results in Figure 3 suggest that there are significant variations in viscosity through the film and this is confirmed by the results shown in Figure 4. The contours depict the shear rate and the corresponding viscosity variation through the nip section. High shear rates are generated in the inlet region and just downstream from the minimum film thickness point. These are a consequence of the pressure gradients that are present at these locations. The pressure gradients lead to a Poiseulle flow component and in the case of rollers having identical surface velocities, only this flow component leads to a shearing action in the film. Thus the highest shear rate occurs near to the roller surface, in this case resulting in 50 per cent change in viscosity over the film thickness. The shear rate contours also illustrate the high levels that are present through the film, even under rolling conditions. This indication is useful as a guide to the level of shear that is required in characterising fluids for these applications. The levels exhibited are within the working limits of rheometers that are commercially available, however when roller speed differentials are present, these rates will become more extreme, possibly

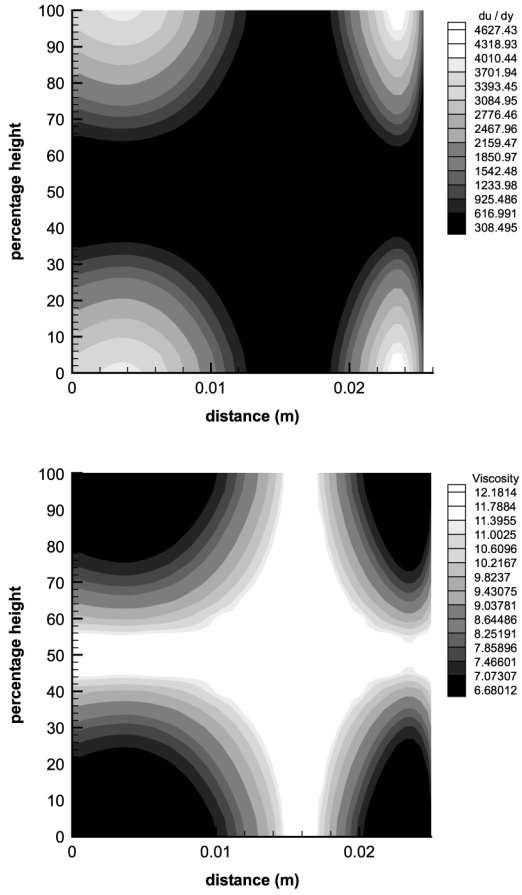

Figure 4.
Shear rate and viscosity variation through the nip section $m = 50$, $n = 0.75$, $U_1 = U_2 = 2.5\,\mathrm{m/s}$

achieving levels that are at the working limits of the most appropriate rheometer systems.

Having explored the comparison between a Newtonian and non-Newtonian model, calculation was completed to investigate the response to changing viscosity coefficient (m) and power law index (n). The viscosity coefficient (m) was varied over the range 30 to 70 Pas and the index (n) from 0.65 to 0.85. The effect of changing the viscosity coefficient is shown in Figure 5. For the prescribed load, this has the most significant impact on the film thickness profile with the more viscous fluid giving a larger film thickness. Similar behaviour has been noted for a Newtonian fluid (Bohan *et al.*, 1997a). The figure also shows that minimum film thickness decreases non-linearly with a proportionate change in viscosity coefficient. A 19 per cent reduction in film thickness occurs when the viscosity changes from 70 Pas to 50 Pas and a drop of 27 per cent in thickness occurs corresponding to a viscosity coefficient

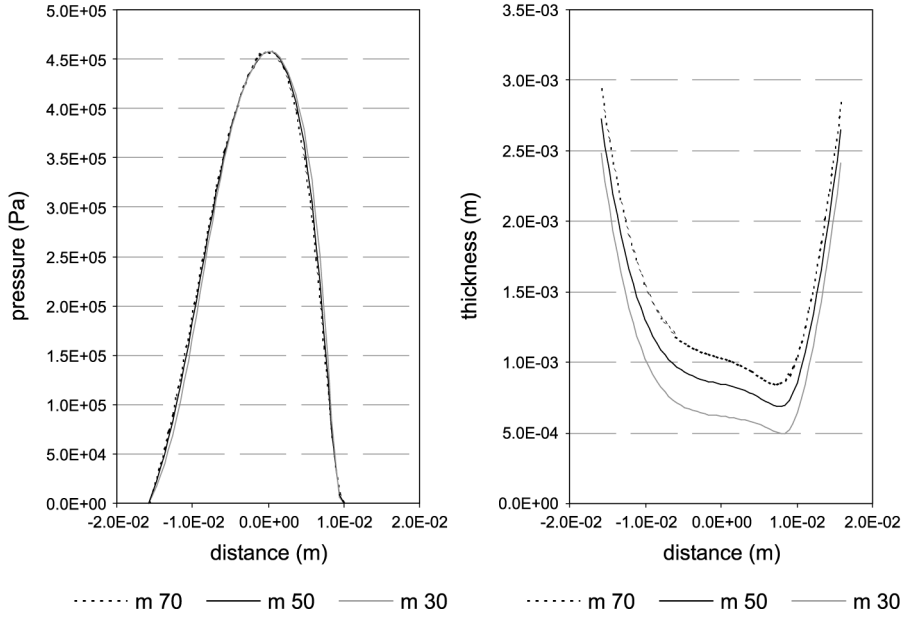

Figure 5.
The influence of viscosity coefficient on pressure and film thickness, $n = 0.75$, $U_1 = U_2 = 2.5\,\mathrm{m/s}$

change from 50 Pas to 30 Pas. This behaviour is a consequence of employing the power law equation to represent viscosity behaviour. At the lower viscosity setting, the film thickness will be affected directly by the value of the viscosity coefficient, however, for the low viscosity, the reduction in film thickness leads to higher shear rates in the film and this exacerbates the viscosity reduction. This mechanism is more dominant at the lower viscosity level and this is reflected in the more marked reduction in film thickness.

Following on from the discussion of the previous case study concerning the direct dependence of pumping capacity on minimum film thickness, this is also reduced in near identical proportions as the viscosity coefficient is dropped from 70 Pas to 30 Pas. From a practical sense this points to a strong requirement to control viscosity closely since this will have a direct impact on the coating film thickness.

The power law exponent represents the degree of shear thinning and the impact of this parameter on nip behaviour is shown in Figure 6. The effect on the form of the pressure profile is similar to that discussed in connection with Figure 3, with the peak value moving towards the nip centre for the more shear thinning fluid. The change in minimum film thickness profile displays the expected form with the higher viscosity fluid increasing the minimum film thickness. However this increase does not depend linearly on the index. This is attributed to the non-linear change in viscosity in response to linear changes in the power law index value. Also since the pumping capacity in the nip depends

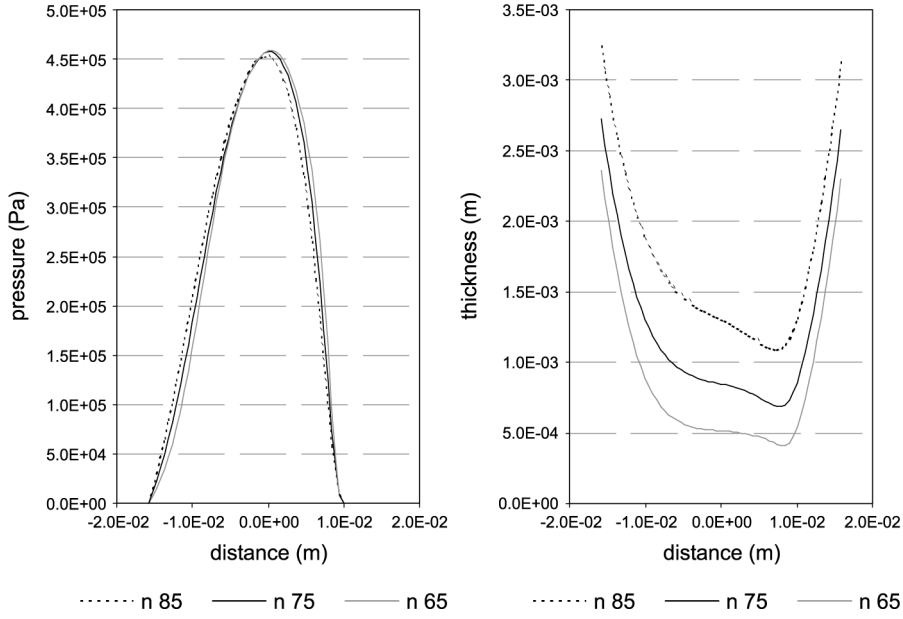

Figure 6.
Influence of power law exponent on pressure and film thickness, $m = 50\,\text{Pas}$, $U_1 = U_2 = 2.5\,\text{m/s}$

on the film thickness at the point of peak pressure, Figure 6 also suggests that the nip pumping capacity is also affected nonlinearly by identical change in power law index value.

As well as determining processing capacity, speed is one of the major control features for coating applications. Through a series of calculations, it was found that the influence of rolling speed on the flow rate per unit width of roller and minimum film thickness is significant and increases non-linearly as depicted in Figure 7. Two mechanisms are present. The first is associated with a simple increase in speed, where, for a constant load application, the film thickness is

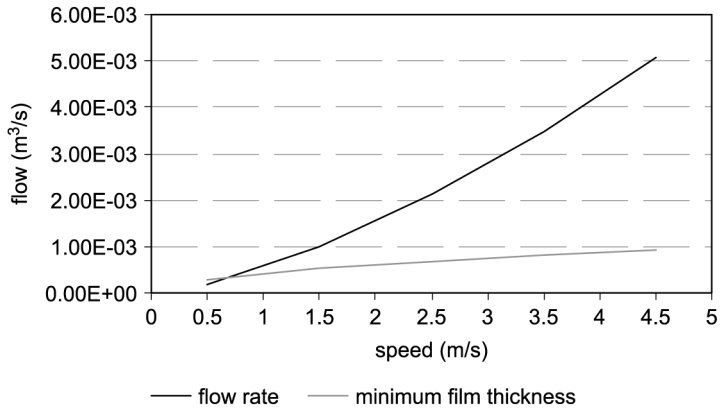

Figure 7.
Influence of speed on flow rate per unit roller width and minimum film thickness, $m = 50\,\text{Pas}$, $n = 0.75$

expected to increase in a linear manner. The second mechanism is more subtle, arising due to the increase in film thickness and the consequent small reduction in shear rate. The latter also leads to a further small increase in viscosity and this will also increase the film thickness. Their combined effect is to increase the film thickness in a nonlinear manner.

The combined effect of higher entrainment velocity together with the non-linear increase in the film thickness gives an increase in calculated flow rate that follows a similar pattern to the film thickness variation. Practically this will be reflected in higher coating weight that can be reduced most directly by increasing the load on the roller pair, or through the application of a speed differential to the rollers forming the nip. The latter will be discussed more fully in a following case study.

Influence of sliding on nip performance

As explained previously, different roller speeds are used as a means of controlling precisely the pumping capacity of the nip, particularly when thin films need to be deposited. The pumping capacity is affected by the combined influence of net entrainment and hydrodynamic action. The latter refers to the pressure field that is generated in the nip and for a given load this will determine the working film thickness in the gap. In the following case studies, the lower roller speed (U_1) is maintained constant and the upper roller speed (U_2) is varied. The consequent effect on film pressure and thickness profile is shown in Figure 8 and the associated viscosity variation through the film section is shown in Figure 9.

As shown in Figure 8, the impact of a sliding component on the shape of the pressure profile is negligible. It has a more significant effect on the minimum film thickness and this is non-linear with respect to the speed increment. As expected, decreasing the upper roller speed by 2 m/s with respect to the lower roller leads to a reduction in film thickness whereas increasing it by an equivalent amount leads to a larger film thickness. However the difference in film thickness does not vary proportionately. For a constant load application, in common with previous discussion, two mechanisms are present. Notably the lower entrainment will lead to a reduction in film thickness due to hydrodynamic action. Since the pressure profiles will be similar in each case to satisfy the load criterion, the Poiseulle flow velocity profile will also be similar. Because the basic film thickness is reduced due to the lower entrainment, this will lead to a higher shear rate through the film. Consequently there will be a further reduction in viscosity. This is confirmed on examining the viscosity contours, Figure 9, where it can be established that the overall effect was to give lower viscosity at low speed and higher viscosity at high speed.

The effect of sliding on the viscosity profiles is shown in Figure 9. These show a significant change from the rolling case, Figure 4, in which there are large zones in which the fluid viscosity is high due to the low velocity

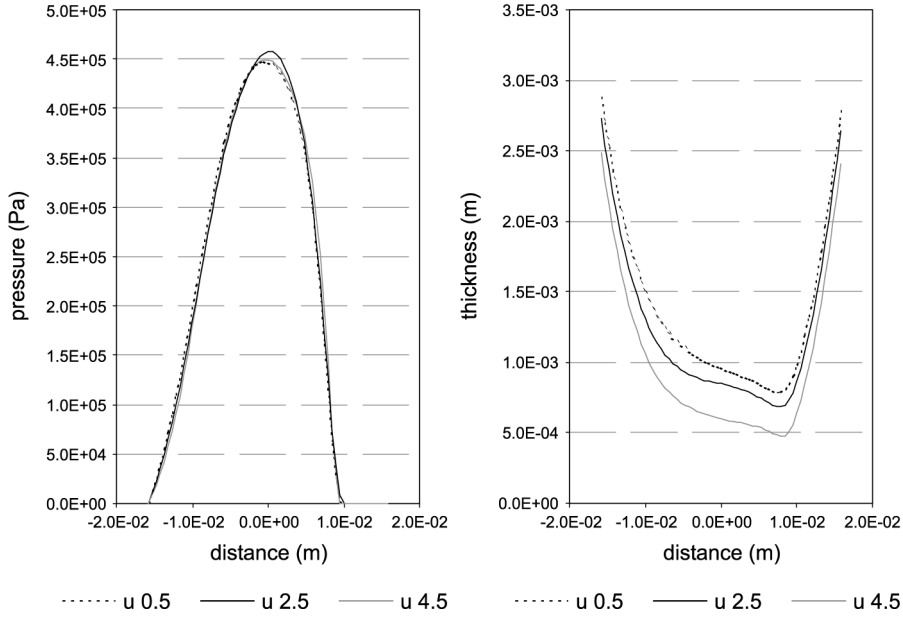

Figure 8.
Influence of sliding on pressure and film thickness, $U_1 = 2.5\,\text{m/s}$, $m = 50\,\text{Pas}$, $n = 0.75$

gradients in these regions. When different roller speeds are present, the velocity gradients are automatically increased and the viscosity field becomes asymmetric with respect to the film centreline. As shown in Figure 9, by changing the upper roller speed from 0.5 to 4.5 m/s the viscosity profile is approximately inverted. However the latter condition leads to a viscosity field that is, on average, higher in value and this affects the nip behaviour in the manner discussed above.

The application of speed differential is used as a precise control to determine the flow rate through the nip. Also the influence of roller speed and speed ratio is important since in combination they determine process through flow and coating weight. The result from a series of calculations in which their combined effect is explored is shown in Figure 10. The characteristics are similar in form with the non-linear increase in flow rate being a combination of film thickness and entrainment velocity. The governing physics has been discussed in connection with Figure 8 and Figure 9. Superimposed are different sliding ratios with the top roller speed (U_2) ranging from half to four times the speed of the bottom roller (U_1). The characteristic shows clearly the application of speed differential in controlling flow through the nip. Fortuitously this control becomes most precise as the upper roller running at speed U_2 decreases below that of the lower roller running at speed U_1 for which the ratio U_1/U_2 exceeds unity. As shown in Figure 10, large changes in relative roller speed in this operating region lead to only small changes in nip pumping capacity.

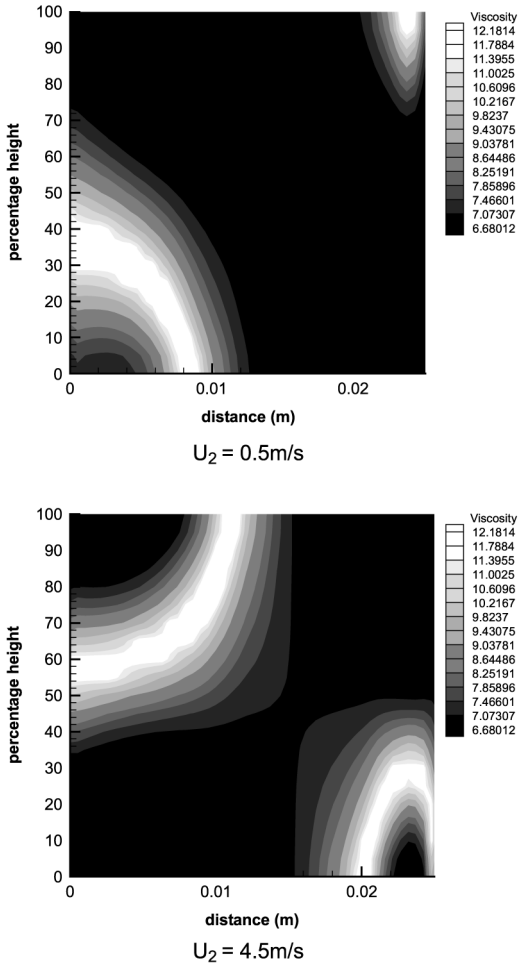

Figure 9.
Viscosity contours through the nip junction, $m = 50\,\text{Pas}$, $n = 0.75$, $U_1 = 2.5\,\text{m/s}$ $U_2 = 0.5\,\text{m/s}$ $U_2 = 4.5\,\text{m/s}$

Conclusions

A fast and computationally efficient model has been developed for a SEHL contact lubricated using a non-Newtonian fluid. This has been effected with the use of a power law fluid. The numerical analysis couples the solution of the generalised pressure equation and those of the elastomer and incorporates the non-Newtonian behaviour in the generalised pressure equation. A sensitivity study has been completed to establish the impact of rheology and speed on the film thickness and pumping capacity within the nip operating in pure rolling and under combined rolling/sliding conditions.

From this work it may be concluded that for SEHL problems, significant differences occur in the nip performance between the Newtonian and non-Newtonian fluids. For shear thinning fluids the high shear in the nip cause a

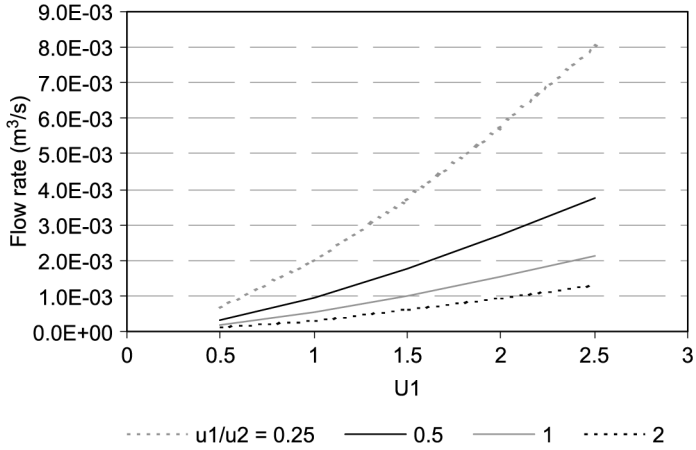

Figure 10.
Relationship between speed, sliding ratio and flow rate per unit roller width, $m = 50$ Pas, $n = 0.75$

drop in the local viscosity. This change in the fluid properties leads to a reduction in the film thickness and for the peak pressure to move closer to the centre of the nip.

With regard to fluid properties, reducing either the viscosity coefficient (m) and power law index (n) results in a reduction of the minimum film thickness with an associated reduction in the flow rate through the nip. The pressure profiles, for a constant load case, are also altered slightly with the peak pressure moving towards the centre of the nip.

In sliding, the shear rate and viscosity profiles become asymmetric. For a constant nip load, the lower entrainment leads to lower viscosity since the film thickness is reduced and the shear rates increase as a consequence. The opposite effect is observed for the higher entrainment. Roller speed has been shown to have a large impact on the flow rate and film thickness, causing increases for all roller speed ratios. For a fixed load, the increased speeds increase the film thickness and reduce the shear rate as a consequence. The combined effect is a non-linear increase in the nip pumping capacity.

For constant load, speed differential is very effective in controlling nip pumping capacity and the system response is particularly sensitive at the lower entrainment speed.

References

Banerjee, P.K. and Butterfield, R. (1981), *Boundary element method in engineering science*, McGraw Hill, New York.

Bennett, J. and Higginson, G.R. (1970), "Hydrodynamic lubrication of soft solids", *Proc. I.Mech.E. Journal of Mechanical Engineering Sciences*, 12, pp. 218-22.

Brebbia, C.A. and Dominguez, J. (1989), *Boundary elements: An introductory course*, McGraw Hill.

Bohan, M.F.J., Claypole, T.C., Gethin, D.T. Basri, S.B. (1997), "Application of boundary element modelling to soft nips in rolling contact" 49th TAGA Tech. Conf., Quebec, May.

Bohan, M.F.J., Lim, C.H., Korochkina, T.V., Claypole, T.C., Gethin, D.T. and Roylance, B.J. (1997b), "An investigation of the hydrodynamic and mechanical behaviour of a soft nip in rolling contact", *Proc. IMechE part J*, 211 No. J1, pp. 37-50.

Cudworth, C.J., "Finite Element Solution of the Elastohydrodynamic Lubrication of a Compliant Surface in Pure Sliding", 5th Leeds-Lyon Symposium on Tribology, Leeds, 1979.

Carvalho, M.S. and Scriven, L.E. (1997), "Deformable roller coating flows: steady state and linear perturbation analysis", *Journal of Fluid Mechanics*, 339, pp. 143-72.

Dowson, D. (1962), *A Generalised Reynolds Equation for Fluid Film Lubrication; International Journal of Mechanical Engineering Sciences.*, 4, pp. 159-70.

Dowson, D. and Ehret, P. (1999), "Past present and future studies in elastohydrodynamics", *Proc I Mech E (J)*, 213, pp. 317-33.

Dowson, D. and Higginson, G.R. (1959), "A numerical solution to the elastohydrodynamic Problem", *J. Mech. Eng. Sci.*, 1, pp. 6-15.

Hannah, M. (1951), "Contact stress and deformation in a thin elastic layer", *Quarterly Journal of Mechanics and Applied Maths*, 4, pp. 94-105.

Hooke, C.J. (1986), "The elastohydrodynamic lubrication of a cylinder on an elastomeric layer", *Wear*, 111, pp. 83-99.

Hooke, C.J. and O'Donoghue, J.P. (1972), "Elastohydrodynamic lubrication of soft, highly deformed contacts", *Proc. I.Mech.E., Journal of Mechanical Engineering Sciences*, 14, pp. 34-48.

Jacobson, B.O. and Hamrock, B.J. (1984), "Non-Newtonian fluid model incorporated into elastohydrodynamic lubrication of rectangular contacts", *Trans. ASME (JOLT)*, 106, pp. 275-84.

Kistler, S.F. and Schweizer, P.M. (1997), *Liquid Film Coating*, Chapman and Hall.

Lim, C.H., Bohan, M.F.J., Claypole, T.C., Gethin, D.T. and Roylance, B.J. (1996), "A finite element investigation into a soft rolling contact supplied by a non-newtonian ink", *J. Phys. D: Appl. Phys*, 29, pp. 1894-903.

Miller, R.D.W. (1966), "Some effects of compressibility on the indentation of a thin elastic layer by a smooth rigid cylinder", *Applied Scientific Research*, 16, pp. 405-24.

MacPhee, J., Shieh, J. and Hamrock, B.J. (1992), "The application of elastohydrodynamic lubrication theory to the prediction of conditions existing in lithographic printing press roller nips", *Advances in Printing Science and Technology*, 21, pp. 242-76.

Parish, D.J. (1958), "Apparent slip between metal and rubber covered pressure rollers", *Bri. J. Appl. Maths*, 9, pp. 428-33.

Walters, K. (1975), *Rheometry*, Chapman and Hall.

Wilkinson, W.L. (1960), *Non-Newtonian Fluids – Fluid Mechanics, Mixing and Heat Transfer*, Pergamon Press Ltd.